Progress In Electromagnetics Research C, Vol. 3, 103–117, 2008

INVESTIGATION OF OPTICAL PROPERTIES OF SI-NC ER-DOPED FIBER AMPLIFIER WITH THE GAUSSIAN RADIUS DISTRIBUTION OF NC

S. Ahmadian and H. G. Fard

Faculty of Electrical Engineering
Amirkabir University of Technology
Tehran, Iran

A. Rostami †

Photonics and Nanocrystal Research Lab. (PNRL)
Faculty of Electrical and Computer Engineering
University of Tabriz
Tabriz, Iran

Abstract—Optical and electrical properties of Er-doped Si-nanocrystal (Si-NC) fiber amplifier are studied. Presence of Si-NC near Er^{3+} ions in silica matrix induces strong coupling mechanism and improves the efficiency of Er^{3+} excitation but in this process the size of Si-NC is important. We investigate effect of radius variation of Si-NC in the range of 2–6 nm by studying the steady state and time resolved luminescence signals at 1.54 μm. We conclude that by limiting the range of Si-NC sizes the amplifier gain is improved. On the other hand Si-NCs may introduce optical loss mechanism, such as confined carrier absorption loss that affects the possibility of obtaining positive net gain. But this detrimental event can be affected by change in the radius of Si-NC as reported in this article.

1. INTRODUCTION

Erbium-doped fiber amplifier is used in optical telecommunication technology as an amplification medium. Er^{3+} ions exhibit a number of emission lines due to electronic transitions from first excited

† Also with School of Engineering Emerging Technologies and Center of Excellence for Mechatronics, University of Tabriz, Tabriz 51664, Iran

state to ground state at $1.54\,\mu$m a standard wavelength in optical telecommunication.

Optical amplification at this wavelength can be achieved if sufficient Er ions can be brought into the first excited state. Unfortunately, the optical cross sections are small, typically in the order of $10^{-21}\,\mathrm{cm}^2$. For this reason there is considerable interest in sensitizing the Er^{3+} ions by adding a strongly absorbing species such as Si-nanocrystals that can transfer energy efficiently to Er. Silicon nanocrystals are formed in SiO_2 using ions implantation followed by thermal annealing. Si nanocrystals (Si-NC) in silica matrices have revealed as efficient sensitizers for Er^{3+} based on the following reasons.

1) Their absorption cross section ($10^{-16}\,\mathrm{cm}^2$ at 488 nm for low pumping power) is more than two orders of magnitude higher than that of Er^{3+} in SiO_2 ($10^{-21}\,\mathrm{cm}^2$ at 980 nm) [3],

2) The decay channels typically limiting the efficiency of Er emission in crystalline Si are absent in this case [1–4].

The recent determination of net optical gain at $1.54\,\mu$m in Er-doped Si-NC sensitized waveguides and the demonstration of efficient room temperature electro luminescence from Er-Si NC devices [1, 5, 6] opened the route towards the future fabrication of electrically driven optical amplifiers based on this system. In coupled Si-NC fibers (EDFA), Er^{3+} ions present an enhancement of the effective excitation cross section up to $10^{-16}\,\mathrm{cm}^2$ [1], quantum efficiency greater than 60% and Si-NC to Er^{3+} transfer rates higher than $1\,\mu\mathrm{m}^{-1}$ by pumping at 488 nm at low fluxes [5], but strong detrimental processes such as cooperative up-conversion (related to Er content), Auger non-radiative de-excitations and confined carrier absorption (CA) within the Si-NC are preventing net optical gain when reaching higher pumping fluxes [6, 7]. It is worth to note that CA has not only the effect of introducing a pump power dependent loss mechanism at the signal wavelength but also of decreasing the effective excitation cross section of Er^{3+} by introducing a competing mechanism for Si-NC de-excitation. The optimum energy transfer from Si-NC to depends on Si-NC sizes and density of Si-nc's and Er^{3+} ions in silica matrices. High density of Si-NC is desired to efficiently pump all the Er^{3+} ions, but this high density will in turn causes a significant CA and will affect optical losses.

In this work, we assume that the density of Si-NC has value of $\sim 1 \times 10^{19}/\mathrm{cm}^3$, but the radius of Si-NC changes within the range of 2∼6 nm. In the present paper, we investigate the effect of Si-NC's size on optical properties of silicon nanocrystal doped EDFA, and through a comparison of simulated photo-luminescence data in a wide range of Er concentrations and pump power, both the coupling and the up-conversion effects will be determined.

Organization of the paper is as follows.

In Section 2, modeling of Si-NC-Er doped fiber from interaction between ions is presented and discussed. Rate equation for description of light amplification is presented in Section 3. Simulation results of proposed model are illustrated in Section 4. Finally the paper ends with a short conclusion.

2. MODELING SI-NANOCRYSTAL-ER INTERACTION

Fig. 1 shows the electronic band structure of Si-NC-doped SiO_2 and Er energy levels. Pump photons are absorbed by introduced confined exciton in Si-NC. The excitonic energy due to the recommendation of confined exciton is transferred to the nearby erbium ion by means of a resonant non-radiative transfer mechanism. Er ion excited to $4I_{11/2}, 4I_{9/2}$ or $4F_{9/2}$ energy levels depend on Si-NC's size and band gap. From those energy levels, the Er^{3+} ion relaxed quickly and non-radiatively to $4I_{13/2}$ energy level. Relaxation of Er^{3+} ions from this level to ground state accurse radiatively with $\lambda = 1.54\,\mu$m, which amplified the standard wavelength [2]. In this simulation, we will consider that radius of Si-NCs various within range 2–6 nm. Both experimental and theoretical studies revealed that a decrease in cluster size induced longer confinement energy and therefore band gap is increased. With perfectly spherical Si-NC with radius R, the following relations based on quantum mechanical relations can be obtained.

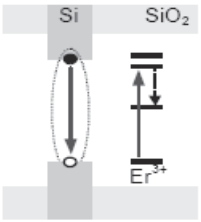

Figure 1. Schematic band structure of an Er doped Si nanocrystal in SiO_2.

The electron energy is given by:

$$E^e_{n,l} = E^c + \frac{\hbar^2}{2m^*_e}\left(\frac{\chi_{n,l}}{R}\right)^2 \tag{1}$$

and the hole energy is obtained as follows:

$$E^h_{n,l} = E^v + \frac{\hbar^2}{2m^*_h}\left(\frac{\chi_{n,l}}{R}\right)^2 \tag{2}$$

Therefore, the energy band gap is:

$$E_{gap} = E_{gap}^{(0)} + \frac{\hbar^2}{2}\left(\frac{\chi_{n,l}}{R}\right)^2\left(\frac{1}{m_e^*} + \frac{1}{m_h^*}\right), \tag{3}$$

where n, l are non-zero positive integers, $\chi_{n,l}$ is the nth zero of the Bessel function, $J_l, E_{gap}^{(0)}$ is the energy gap in bulk silicon and it is approximately equal to 1.12 eV. Also, m_e^* and m_h^* are the effective electron and hole masses respectively [2]. For 2–6 nm Si-NC's size variation the band gap range is from 2.08 to 1.22 eV. By considering the energy level of Er^{3+}, the effective energy transfer from Si-NC to Er^{3+} can be happen for 2.2 nm, 3 nm and 5.2 nm radius sizes only for uniform Si-NC distribution along the fiber with density of $1 \times 10^{19}/\text{cm}^3$ as an example. Radius probability distribution is assumed to be Gaussian for Si-NCs. The mean value of this function assumed to be 3 nm for simulation purposes.

$$F(r) = \frac{1}{\sqrt{2\pi}\delta} e^{-\frac{(r-3)^2}{2\delta^2}} \tag{4}$$

In order to compute total gain, we should multiply the gain of each case to its probability function, sum of them result the total gain of amplifier.

$$Gain = \sum_i F_i G_i \tag{5}$$

3. RATE EQUATIONS

In order to describe the considered amplifier, we consider the Si-NC as an effective two-level system, where the ground state is represented by level a and the excited state by level b. Thus δ_{ab} is the effective excitation cross section describing the creation of an exciton and its subsequent fast trapping at the interfacial level, following the absorption of a 488 nm pump photon. W_b is the total recombination rate of an exciton for the isolated Si-NC comprising both radiative and non-radiative recombination rates. The considered Er^{3+} ions are assumed a five levels system. With given W_{ij}, we indicate the total transition rate from level i to level j, where $i, j = 1 - 5$ and $i > j$.

One of most important coefficients is C_{b1} which it describes the coupling between the excited state of Si-NC and the ground state of Er^{3+} ions, C_{bi} $(i \geq 2)$ describes the excited state excitation (ESE) from level i to level b. In this case, ESE describes the re-excitation of excited Er^{3+} ions through the energy transfer from an excited Si-NC.

Another effect which we should take into account is very similar to the Auger effect occurring in Er-doped crystalline Si that cause the energy transferred from excited Er ions back to a confined exciton, thus promoting it to a higher energy level. This process is represented by the constant CA. We also take into account the concentration quenching effect (W_{er}), which is due to the energy migration all over the sample caused by the energy transfer between two nearby Er^{3+} ions, one in the first excited level and the other in the ground state, $W_{er} = 8.1 \times 10^{-19} N_0 S^{-1}$ which N_0 is the total Er concentration. The constants C_{up} and C_3 are the cooperative up-conversion coefficients describing the interaction of two nearby Er ions which are either in the first or in the second excited states, respectively. In first case (ground state) giving its energy to the other which will be excited to the third excited level. In the second case the interaction will bring one ion to the fifth level and the other to the ground state. In the model, we take also into account the possibility of a direct absorption of a 488 nm photon by Er ions leading to a transition from the ground state to fifth level. This process is characterized by an excitation cross section of $\sim 1 \times 10^{19}\,\mathrm{cm}^2$.

Now, we are able to write down sets of first order rate equations describing the time evaluation of the concentration of Si-NC and Er ions in each level. We assume that all coefficients in these equations are constant respect to Si-NC radius. Then rate equations for Si-NC are:

$$\frac{dn_b}{dt} = \delta_{ab}\varphi n_a - w_b n_b - \sum_{i=1}^{3} C_{bi} n_b N_i \tag{6}$$

$$\frac{dn_a}{dt} = -\delta_{ab}\varphi n_a + w_b n_b + \sum_{i=1}^{3} C_{bi} n_b N_i \tag{7}$$

For energy transfer from 2.2 nm Si-NC to Er^{3+} ion the rate equations are:

$$\begin{aligned}
\frac{dN_5}{dt} &= \delta\varphi N_1 + \sum_{i=1}^{3} C_{bi} n_b N_i + C_3 N_3^2 - w_{54} N_5, \\
\frac{dN_4}{dt} &= C_{up} N_2^2 + w_{54} N_5 - w_{43} N_4, \\
\frac{dN_3}{dt} &= w_{43} N_4 - (w_{32} + w_{31}) N_3 - C_{b3} n_b N_3 - 2C_3 N_3^2, \\
\frac{dN_2}{dt} &= w_{32} N_3 - (w_{21} + w_{er}) N_2 - 2C_{up} N_2^2 - C_{b2} n_b N_2 - C_A n_b N_2,
\end{aligned} \tag{8}$$

$$\begin{aligned}\frac{dN_1}{dt} &= (w_{21}+w_{er})N_2 - C_{up}N_2^2 + C_A n_b N_2 \\ &\quad + w_{31}N_3 + C_3 N_3^2 - C_{b1}n_b N_1 - \delta\varphi N_1,\end{aligned}$$

For 3 nm Si-NC the rate equations of Er^{3+} are:

$$\begin{aligned}\frac{dN_5}{dt} &= \delta\varphi N_1 + \sum_{i=2}^{3} C_{bi}n_b N_i + C_3 N_3^2 - w_{54}N_5, \\ \frac{dN_4}{dt} &= C_{b1}n_b N_1 + C_{up}N_2^2 + w_{54}N_5 - w_{43}N_4, \\ \frac{dN_3}{dt} &= w_{43}N_4 - (w_{32}+w_{31})N_3 - C_{b3}n_b N_3 - 2C_3 N_3^2, \\ \frac{dN_2}{dt} &= w_{32}N_3 - (w_{21}+w_{er})N_2 - 2C_{up}N_2^2 - C_{b2}n_b N_2 - C_A n_b N_2, \\ \frac{dN_1}{dt} &= (w_{21}+w_{er})N_2 - C_{up}N_2^2 + C_A n_b N_2 \\ &\quad + w_{31}N_3 + C_3 N_3^2 - C_{b1}n_b N_1 - \delta\varphi N_1,\end{aligned} \tag{9}$$

and for 5.2 nm Si-NC, we can write:

$$\begin{aligned}\frac{dN_5}{dt} &= \delta\varphi N_1 + \sum_{i=2}^{3} C_{bi}n_b N_i + C_3 N_3^2 - w_{54}N_5, \\ \frac{dN_4}{dt} &= C_{up}N_2^2 + w_{54}N_5 - w_{43}N_4, \\ \frac{dN_3}{dt} &= C_{b1}n_b N_1 + w_{43}N_4 - (w_{32}+w_{31})N_3 - C_{b3}n_b N_3 - 2C_3 N_3^2, \\ \frac{dN_2}{dt} &= w_{32}N_3 - (w_{21}+w_{er})N_2 - 2C_{up}N_2^2 - C_{b2}n_b N_2 - C_A n_b N_2, \\ \frac{dN_1}{dt} &= (w_{21}+w_{er})N_2 - C_{up}N_2^2 + C_A n_b N_2 \\ &\quad + w_{31}N_3 + C_3 N_3^2 - C_{b1}n_b N_1 - \delta\varphi N_1,\end{aligned} \tag{10}$$

where φ is the flux of photons incident on to the sample. In these relations $n_{a,b}$ and N_i, with $i \geq 1$ are density level populations of Si nanocrystal and of Er ions. In particular, we can define $n_a + n_b = n_0$ and $\sum N_i = N_0$, where n_0 and N_0 are total concentrations of excitable Si-NC's and Er ions, respectively.

4. SIMULATION RESULTS

In this section we want to investigate the gain and other optical properties of Er-doped Si nanocrystals. The physical variables that

have been varied in the investigation are the Er concentration (varying between $1 \times 10^{17}\,\mathrm{cm}^{-3}$ and $9 \times 10^{22}\,\mathrm{cm}^{-3}$) and the excitation pump photons (in the range $1 \times 10^{17} - 9 \times 10^{22}\,\mathrm{cm}^{-2}\mathrm{sec}^{-1}$). The density of Si-NC's in the sample has been fixed to $1 \times 10^{19}\,\mathrm{cm}^{-3}$.

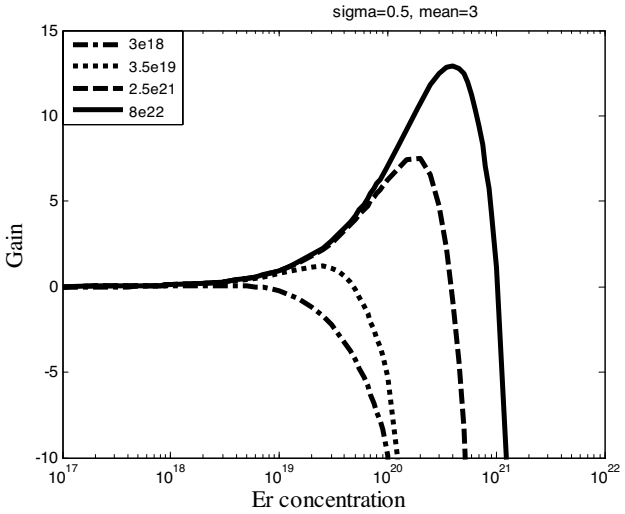

Figure 2. Gain vs. Er concentration, pump photons: $3 \times 10^{18}, 3.5 \times 10^{19}, 2.5 \times 10^{21}$ and $8 \times 10^{22}\,\mathrm{cm}^{-2}\mathrm{sec}^{-1}$, δ: 0.5 nm and mean value: 3 nm.

Fig. 2 illustrates optical gain versus concentration of Er ions for different pump intensity levels in steady state condition where the value of δ equal to 0.5. Actually gain $= \delta_e(N_2 - N_1)$ where δ_e is the emission cross section of level $4I_{13/2}$, and $(N_2 - N_1)$ is the total concentration of Er ions inverted in that level. For the emission cross section of Er, a value of $1 \times 10^{-19}\,\mathrm{cm}^2$ has been used [1]. Starting from a value of $1 \times 10^{17}\,\mathrm{cm}^{-3}$, the value of pump power needed to have positive gain has to be increased too. It is worth to note that for Er concentrations higher that the Si-NC is, despite quenching processes limit the gain. Fig. 3 shows the gain vs. photon flux for some Er concentration. It is observed that in high pump intensity with increasing Er ions concentrations the value of gain is increased. In particular, higher Er induced gain can be reached at the highest pump powers and Er concentrations. But, what is the effect of the variable δ (variance of Gaussian distribution function) in gain determination?

In Fig. 4 the optical gain versus Er concentration for different δ values is illustrated. It is perceived that with decreasing in value of δ the gain peak is increased. This event is quite interesting, for example

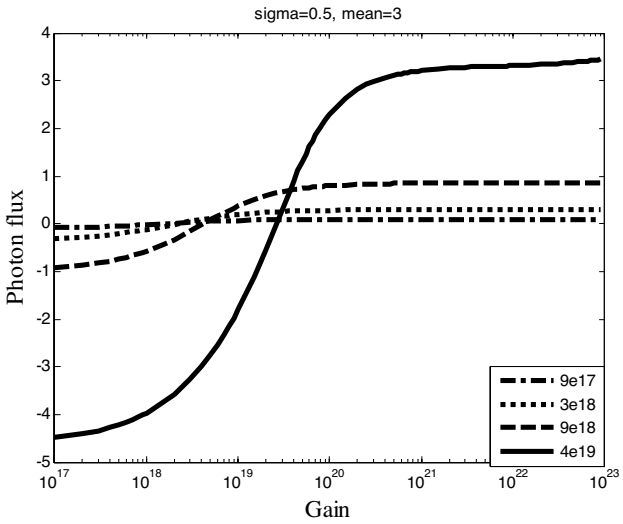

Figure 3. Gain vs. photon flux, Er concentration: $9 \times 10^{17}, 3 \times 10^{18}$, and $4 \times 10^{19}\,\mathrm{cm}^{-3}$, δ: 0.5 nm and mean value: 3 nm.

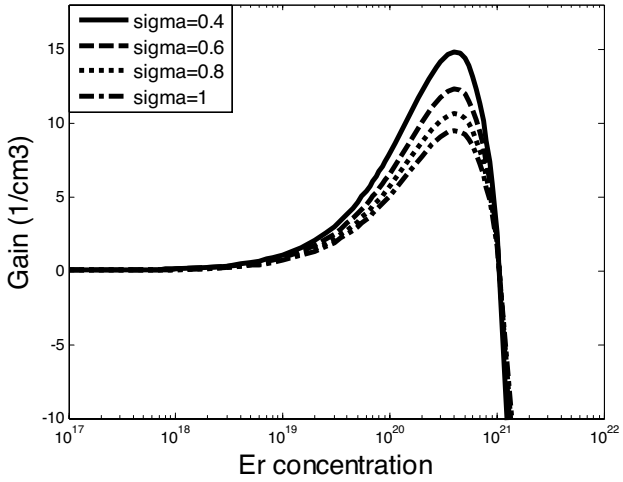

Figure 4. Gain vs. Er concentration: $\delta : 0.4, 0.6, 0.8$ and 1, photon flux: $9 \times 10^{22}\,\mathrm{cm}^{-2}\mathrm{sec}^{-1}$, mean value: 3 nm.

the peak of optical gain for $\delta = 0.8$ is about 11 but for $\delta = 0.4$ is about 15 (in pump photon $9 \times 10^{22}\,\mathrm{cm}^{-3}$). This means that if the size range of Si nanocrystal's limited, the coupling between Si-NC's and Er ions becomes better. Despite the clear positive effects in the Er induced

gain, Si-NC's could, however introduce loss mechanism. The most important loss is the confined carrier's absorption (CCA) mechanism, describing the absorption of a 1.54 μm photon from a confined exciton in a Si-NC. In order to study the weight of CCA, we simulated the fraction of excited Si-NC's in steady state in our Er-doped Si-NC system. By solving Eqs. (6)–(10) and using the coefficients given in the Table 1, we determine the concentration n_b of excited Si-NC's. In Fig. 5 concentration of excited nanocrystals n_c (n_b) is reported as a function of Er concentration for some photon fluxes.

Table 1. Physical parameters [1].

Symbol	Value	Unit
λ	488	nm
δ_{ab}	2×10^{-16}	cm^2
δ	1×10^{-19}	cm^2
w_b	2×10^{4}	s^{-1}
w_{er}	$8.1\times10^{-19}N_0$	s^{-1}
w_{21}	4.2×10^{2}	s^{-1}
w_{32}	4.2×10^{5}	s^{-1}
w_{43}	$\approx1\times10^{7}$	s^{-1}
w_{54}	$\langle1\times10^{7}$	s^{-1}
C_{b1}	3×10^{-15}	$cm^3 s^{-1}$
C_{up},C_3	7×10^{-17}	$cm^3 s^{-1}$
C_{b2},C_{b3},C_A	$\rangle3\times10^{-19}$	$cm^3 s^{-1}$

It is worth noticing that when the concentration of Er ions is lowered than $10^{19}\,\mathrm{cm}^{-3}$, by increasing the pump power, the excited Si-NC's increase in a way which is almost independent of the particular Er concentration. At the pump power used, almost 100% of Si-NC's can be excited. When the Er concentration is increased, more than one Er ion can be coupled with a single Si-NC. Due to the strong coupling, the concentration of Si-NC in excited level decreases. To achieve the CCA losses we need δ_{cca}, the confined carrier absorption cross section, but the exact value of this parameter is not determined up to now. We use the experimental value, $1 \times 10^{-18}\,\mathrm{cm}^2$ reported in [1].

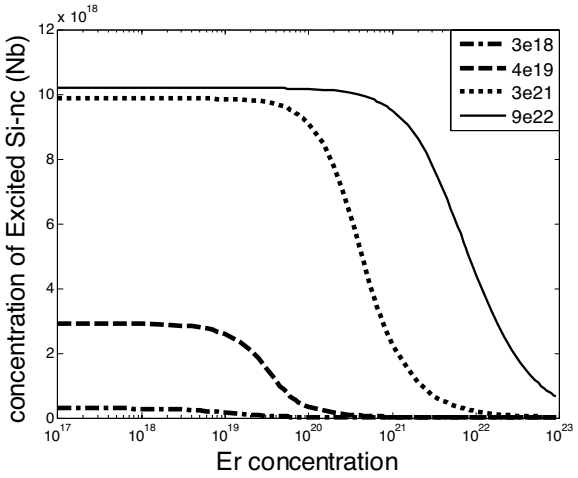

Figure 5. Concentration of excited Si-NC vs. Er concentration, pump photon flux: $3\times10^{18}, 4\times10^{19}, 3\times10^{21}$ and $9\times10^{22}\,\mathrm{cm}^{-2}\mathrm{sec}^{-1}$, δ: 0.5 nm and mean value: 3 nm.

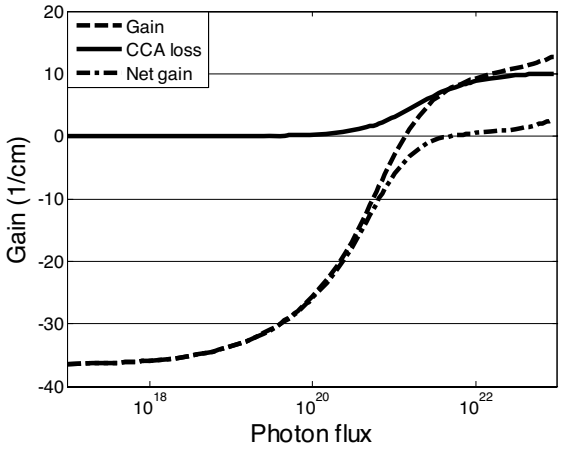

Figure 6. Gain, CCA loss and net gain vs. photon flux, Er concentration: $3\times10^{20}\,\mathrm{cm}^{-3}$, sigma: 0.5 nm, mean value: 3 nm.

The Si-NC induced losses defined by following equation:

$$\alpha_{CCA} = \delta_{CCA} n_b \tag{11}$$

Fig. 6 reports Er induced gain g, the Si-NC induced losses α_{CCA} and effective gain, $g_{net} = g - \alpha_{CCA}$ as a function of excitation photons for

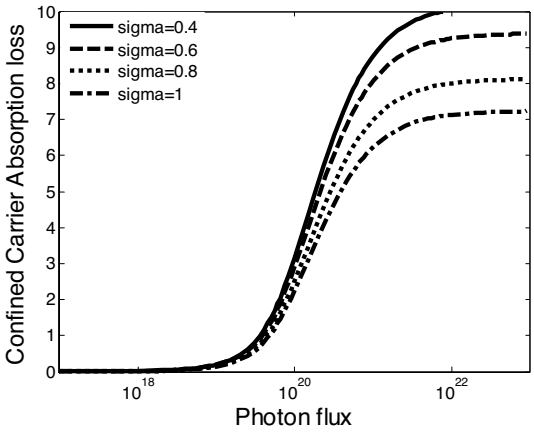

Figure 7. Confined carrier absorption loss vs. photon flux, sigma: 0.4, 0.6, 0.8 and 1, Er concentration: $4 \times 10^{19}\,\mathrm{cm}^{-3}$, mean value: 3 nm.

given Er concentration of $3 \times 10^{20}\,\mathrm{cm}^{-3}$. This positive net gain is a result of sensitizing action played by Si-NC's to excite more than one Er ions; the material gain can be so high to overcome the Si-NC induced losses. With increasing variable δ (variance of Gaussian distribution function) the confined carrier absorption loss decreases (Fig. 7), but as already reported the gain deceases too. Then the net gain of Er-doped Si nanocrystals reduced the undesirable process. So widening the range of the Si-NC's sizes hasn't got favorite effect on the net gain.

Another important factor that we intend to investigate is the life time and frequency response of Si nanocrystal-Er doped amplifier that can be gain by looking at time evolution of the $1.54\,\mu$m emission. Indeed, in Fig. 8 time decay curves recorded at $1.54\,\mu$m are reported for different pump powers, normalized to the steady state values. At $t = 0$, after the system has reached the steady state conditions, we switch off laser beam and measure the time evolution of the luminescence signal. At very low pump power the measured life time is of the order of 1 msec. Actually this low value is a consequence of the concentration quenching effect taking place in this system. With increasing the pump power, a shortening of the measured lifetime is observed in the first instants of the decay, causing a stretching of the decay curve which recovers its original straight shape only at longer times. Indeed, with increasing the pump power, the concentration of Er ions brought into the first excited level in steady state conditions increases too. Hence it becomes more probable to find all over the sample pairs of nearby excited Er ions. Within each pair of excited Er ions a strong cooperative up-conversion

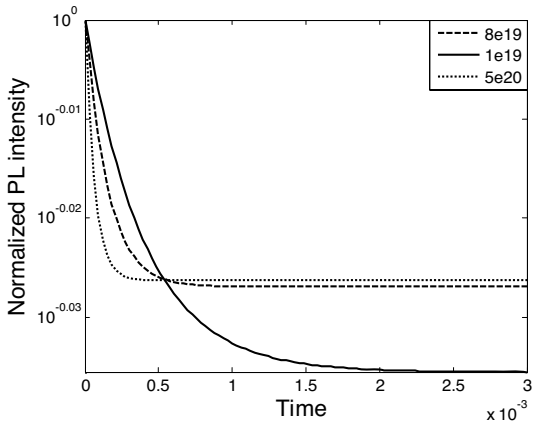

Figure 8. Time decay curve of normalized PL intensity pump photon flux: $1 \times 10^{19}, 8 \times 10^{19}$ and $5 \times 10^{20}\,\mathrm{cm}^{-2}\mathrm{sec}^{-1}$, Er concentration: $5 \times 10^{20}\,\mathrm{cm}^{-3}$, sigma: 0.5, mean value: 3.

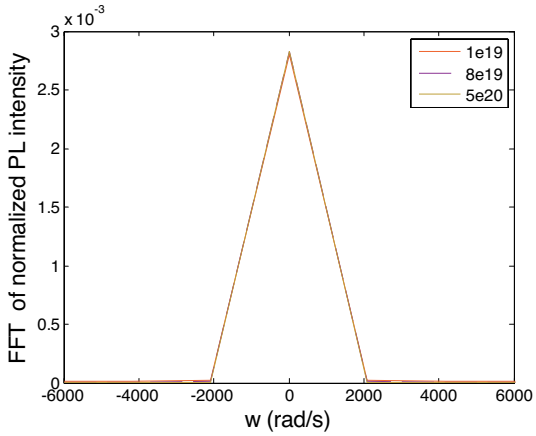

Figure 9. Fast Fourier Transform of normalized PL intensity pump photon flux: $1\times10^{19}, 8\times10^{19}$ and $5\times10^{20}\,\mathrm{cm}^{-2}\mathrm{sec}^{-1}$, Er concentration: $5 \times 10^{20}\,\mathrm{cm}^{-3}$, sigma: 0.5, mean value: 3.

mechanism sets in, producing fast quenching of the first excited level population. This quenching continues until excited Er ions remain only far apart, and, being no more interacting, can relax in the ground state emitting photons with the life time measured at low pump power.

This fact can be revealed from frequency response of normalized intensity at $1.54\,\mu$m when the laser beam switched off. In Fig. 9,

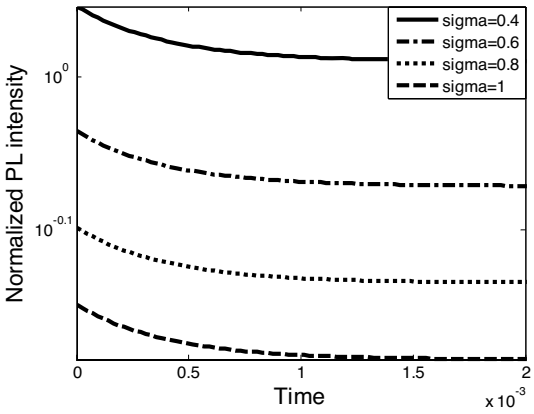

Figure 10. Normalized PL intensity vs. Time δ: 0.4, 0.6, 0.8 and 1, mean value: 3, Er concentration $5 \times 10^{20}\,\mathrm{cm}^{-3}$, pump photon flux $1 \times 10^{19}\,\mathrm{cm}^{-2}\mathrm{sec}^{-1}$.

Fast Fourier Transform of time decay curve of normalized PL intensity depicted for three different pump powers.

Therefore the life time of $1.54\,\mu$m emission photons is independent of pump power. For Er concentration $5 \times 10^{20}\,\mathrm{cm}^{-3}$ and pump photon flux $1 \times 10^{19}\,\mathrm{cm}^{-2}\mathrm{sec}^{-1}$, the band width of frequency response is about 2000 rad/s. We can also draw the time decay curve as a function of δ. In Fig. 10 you can see the normalized PL intensity for δ: 0.4, 0.6, 0.8 and 1. It is observed that by increasing the value of δ, the life time of excited photon on first excited level of Er does not change, only the value of normalized intensity changes.

5. CONCLUSION

We have presented a phenomenological description of the Er-doped Si nanocrystal system. By introducing the rate equations, describing the density populations of interacting Si-NC-Er levels, we were able to investigate the effect of Si-NC's sizes on the gain, confined carrier absorption loss and frequency response of that system. It has been demonstrated that with a narrow range for Si-NC's radius about critical radius (3 nm), we obtain gain about 15, which is more desirable. We have shown that Si-NC's can have positive as well as negative aspects as far as the optical gain at $1.54\,\mu$m from Er-doped Si-NC is concerned. All of this studies, have shown that Er excitation via Si nanocrystals can satisfy all requirements to be used in broadband pumped integrated optical waveguide amplifiers operating at $1.54\,\mu$m.

REFERENCES

1. Pacifici, D., G. Franzo, F. Priolo, F. Lacona, and L. D. Negaro, "Modeling and perspective of the Si nanocrystal Er interaction for optical amplifier," *Phys. Review*, Vol. B67, 45301, 2003.
2. Lucalrz, F., "Sillicon nanocrystal in Er doped silica for optical amplification," Ph.D. Thesis, August 2003.
3. Daldosso, N., D. Navarro, M. Melchiorri, P. Pellegrino, B. Garrido, C. Sada, G. Battaglin, F. Gourbilleau, R. Rizik, and L. Pavaessi, "Er coupled Si nanocluster waveguide," *IEEE Journal in Quantum Electronics*, November 2005.
4. Kik, P. G., M. L. Brangersma, and A. Polman, "Strong exciton-erbium coupling in Si nanocrystal-doped SiO_2," *J. Appl. Phys. Lett.*, Vol. 76, 17, April 2000.
5. Kik, P. G. and A. Polman, "Towards an Er-doped Si nanocrystals sensitized waveguide laser — The thin line between gain and loss," *Towards the First Silicon Laser*, NATO Science Searies II, 93.
6. Kik, P. G. and A. Polman, "Gain limiting process in Er-doped Si nanocrystal waveguides in SiO_2," *J. Appl. Phys.*, Vol. 91, 1, Jan. 2002.
7. Shahoei, H., H. Ghafoori-Fard, and A. Rostami, "A novel design methodology of multi-clad single mode optical fiber for broadband optical networks," *Progress In Electromagnetics Research*, PIER 80, 253–275, 2008.
8. Kamitsos, I. and N. K. Uzunoglu, "Improvement of transmission properties of multimode fibers using spread spectrum technique and a Rake receiver approach," *Progress In Electromagnetics Research*, PIER 76, 413–425, 2007.
9. Singh, S. P. and N. Singh, "Nonlinear effects in optical fibers: Origin, management and applications," *Progress In Electromagnetics Research*, PIER 73, 249–275, 2007.
10. Ikuno, H., S. Mori, and A. Yata, "Uniform asymptotic analysis of guided modes of graded-index optical fibers with even polynomial profile center cores," *Progress In Electromagnetics Research*, PIER 13, 169–241, 1996.
11. Grobe, K. and H. Braunisch, "A broadband model for single-mode fibers including nonlinear dispersion," *Progress In Electromagnetics Research*, PIER 22, 131–148, 1999.
12. Tripathi, R., R. Gangwar, and N. Singh, "Reduction of crosstalk in wavelength division multiplexed fiber optic communication systems," *Progress In Electromagnetics Research*, PIER 77, 367–378, 2007.

13. Rajabvand, M., F. Behnia, and T. M. Fatehi, "Transition region effects in tunable fiber-based wavelength-selective devices," *Progress In Electromagnetics Research*, PIER 82, 33–50, 2008.
14. Shen, G.-F., X.-M. Zhang, H. Chi, and X.-F. Jin, "Microwave/millimeter-wave generation using multi-wavelength photonic crystal fiber Brillouin laser," *Progress In Electromagnetics Research*, PIER 80, 307–320, 2008.
15. Singh, S. P., R. Gangwar, and N. Singh, "Nonlinear scattering effects in optical fibers," *Progress In Electromagnetics Research*, PIER 74, 379–405, 2007.